Author/s:
Morgan, KA;de Veer, M;Miles, LA;Kelderman, CAA;McLean, CA;Masters, CL;Barnham, KJ;White, JM;Paterson, BM;Donnelly, PS

Title:
Pre-targeting amyloid-β with antibodies for potential molecular imaging of Alzheimer's disease

Date:
2023-01-17

Citation:
Morgan, K. A., de Veer, M., Miles, L. A., Kelderman, C. A. A., McLean, C. A., Masters, C. L., Barnham, K. J., White, J. M., Paterson, B. M. & Donnelly, P. S. (2023). Pre-targeting amyloid-β with antibodies for potential molecular imaging of Alzheimer's disease. Chemical Communications, 59 (16), pp.2243-2246. https://doi.org/10.1039/d2cc06850h.

COMMUNICATION

Pre-Targeting Amyloid-β with Antibodies: Toward Antibody Targeted Molecular Imaging of Alzheimer's Disease

Received 00th January 20xx,
Accepted 00th January 20xx

DOI: 10.1039/x0xx00000x

Katherine A. Morgan,[a] Michael de Veer,[b] Luke A. Miles,[c] Cormac A. Kelderman,[d] Catriona A. McLean,[c] Colin L. Masters,[c] Kevin J. Barnham,[c] Jonathan M. White[a], Brett M. Paterson,[b,d] and Paul S. Donnelly*[a]

With the aim of developing the concept of pretargeted click chemistry for the diagnosis of Alzheimer's disease two antibodies specific for amyloid-β were modified to incorporate *trans*-cyclooctene functional groups. Two bis(thiosemicarbazone) compounds with pendant 1,2,4,5-tetrazine functional groups were prepared that were radiolabelled with positron emitting copper-64. The new copper-64 complexes rapidly react with the *trans*-cyclooctene functionalized antibodies in a bioorthogonal click reaction and cross the blood-brain barrier in mice.

Alzheimer's disease (AD) is a progressive neurodegenerative condition that leads to cognitive and behavioural impairment. The pathology of AD is characterised by the presence of both amyloid-β and tau pathology in the brain.[1] The biological impact of amyloid-β plaques and neurofibrillary tau tangles (NFT) is controversial, but the presence of these abnormal protein deposits define AD and form the basis of its differential diagnosis from other dementias.[2,3] A major component of amyloid-β plaques ARE aggregated forms of the amyloid-β peptide (Aβ) which is formed by cleavage of the amyloid precursor protein (APP), a type I transmembrane glycoprotein of 695-770 amino acids.[4] Cleavage of APP leads to the formation of fragments of various lengths with the 40 amino acid variant ($A\beta_{1\text{-}40}$) and 42-amino acid variants, $A\beta_{1\text{-}42}$, both being significant. Aggregation of Aβ leads to the formation of oligomers, protofibrils, fibrils and finally the deposition of extracellular plaques. [4,5]

Positron Emission Tomography (PET) imaging using radiolabelled small molecules that bind to amyloid-β plaques can assist in differential diagnosis of AD.[5] For some patients, amyloid-β burden does not directly correlate with cognitive impairment.[6] This dichotomy has contributed to the theory that soluble Aβ fibrils and oligomers are the neurotoxic species.[7] Current approaches for PET imaging of amyloid-β use small molecules radiolabelled with positron-emitting fluorine-18 that bind to insoluble Aβ plaques. These tracers are typically small aromatic, planar and lipophilic molecules, such as derivatives of stilbenes (florbetapir) or benzothiazoles (flutemetamol). These compounds bind to insoluble amyloid-β plaques through a combination of hydrophobic and non-covalent interactions but offer little insight into the presence of soluble Aβ fibrils and oligomers.[8]

Several anti-Aβ antibodies that target different regions or forms of Aβ have been developed. For example, aducanumab (Aduhelm) is a recombinant IgG1 antibody that binds to soluble Aβ aggregates and insoluble fibrils in preference to monomers.[9] Aducanumab was approved by the FDA in 2021 for the treatment of AD, although the approval was controversial.[10] Diagnostic imaging with radiolabelled antibodies has the potential to offer new insight to conventional amyloid-β plaque imaging. PET imaging with radiolabelled antibodies (immunoPET) has already made a significant impact in the diagnosis of cancer, but the application of immunoPET to diagnose neurodegenerative diseases is challenging. The large molecular weight of radiolabelled antibodies (~ 150 kDa) significantly limits their passage across the blood brain barrier.

In this work, we present an antibody 'pre-target and chase' approach that has the potential to circumvent these challenges (Figure 1). The strategy involves administering an antibody that has been modified to incorporate a functional group poised for a bioorthogonal 'click reaction' with a small molecule radiolabelled tracer that crosses the blood-brain barrier (BBB). The small molecule tracer is administered after allowing sufficient time and repeated dosing to maximise the accumulation of the antibody at the target site in the brain.

Aducanumab crosses the blood-brain barrier and accumulates in the brain of transgenic mice (Tg2576) that are a model of amyloid pathology. Administration of a single dose (30 mg kg^{-1}) to Tg2576 transgenic mice resulted in a C_{max} in brain of 1,062 ng g^{-1} of tissue.[9] Repeated administration of a suitably modified antibody should lead to concentrations in the brain that could be targeted by a radiolabelled small molecule.

The selectivity and fast reaction kinetics (k_2 ~ 10^5 M^{-1} s^{-1}) of inverse-electron-demand Diels-Alder reactions between electron-deficient tetrazines and strained *trans*-cyclooctene (TCO) derivatives are well suited for *in vivo* pre-targeting (Figure 1). Pre-targeting of tumours using antibodies modified to

[a] School of Chemistry and Bio21 Molecular Science and Biotechnology Institute, University of Melbourne, Melbourne, Victoria, 3010, Australia.
[b] Monash Biomedical Imaging, Monash University, Clayton, Victoria 3800, Australia.
[c] The Florey Institute of Neuroscience and Mental Health, University of Melbourne, Melbourne, Victoria, 3010, Australia.
[d] School of Chemistry, Monash University, Clayton, Victoria 3800, Australia.

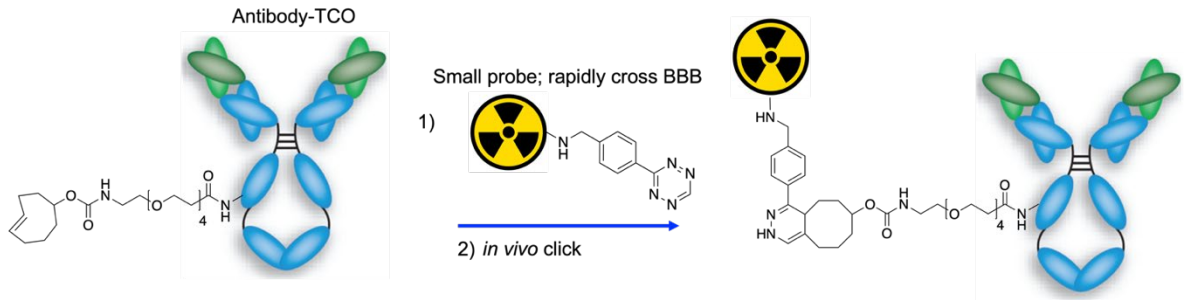

Figure 1 Schematic representation of *in vivo* inverse-electron-demand Diels-Alder 'click' reaction between tetrazines and strained *trans*-cyclooctene (TCO) with a polyethylene glycol linker (PEG_4).

incorporate TCO and radiolabelled molecules featuring a tetrazine has been demonstrated in animal models for both PET imaging and radionuclide therapy.[11] Antibodies that do not internalise upon binding to the antigen are best suited to *in vivo* click reactions,[12] so antibodies such as aducanumab that bind to extracellular soluble Aβ aggregates and insoluble fibrils are well suited for pre-targeted PET-imaging.

In this work, TCO functional groups were conjugated to an aducanumab biosimilar through a short hydrophilic polyethylene glycol (TCO-PEG_4) linker. The antibody was reacted with the succinimidyl ester of TCO-PEG_4-CO_2H (10 equivalents) at room temperature for one hour before purification with an ultra-centrifugation filter (MWCO 50 kDa). Analysis of the aducanumab-PEG_4-TCO conjugates (aducanumab-TCO, Figure 2a) by 'intact' electrospray mass spectrometry (ESI-MS) revealed an average of four PEG_4-TCO groups per antibody. We also added TCO functional groups to the 6E10 antibody, a research anti-Aβ monoclonal antibody that was raised against a synthetic peptide corresponding to residues 1-24 of Aβ.[13] Reaction of 6E10 with the *N*-hydroxysuccinimide activated ester of TCO-PEG_4-CO_2H under the same conditions and analysis by intact electrospray mass spectrometry indicated an average of five PEG_4-TCO groups per antibody (6E10-TCO) (Figure 2b). The more complicated mass spectrum of 6E10-TCO when compared to aducanumab-TCO presumably reflects the higher degree of glycosylation. The modified 6E10-TCO (1:400) retained affinity for Aβ plaques present in post-mortem frontal cortex tissue of subjects with diagnosed AD (Figure 2c) and behaved in the same way as parental 6E10 (1:200, ESI, Figure S21). The binding affinity of the aducanumab biosimilar could not be probed in this manner as the antibody binds to soluble Aβ aggregates. Both aducanumab-TCO and 6E10-TCO were also analysed by size exclusion-HPLC, and the chromatograms were similar to the unmodified antibodies with no evidence of aggregation (ESI, Figure S20).

Copper-64 is a positron-emitting radionuclide that can be used for PET imaging.[14] The copper(II) bis(thiosemicarbazonato) complex diacetyl*bis*(4-methyl-3-thiosemicarbazone) (Cu(atsm), Figure 3a) is charge neutral, lipophilic and is capable of crossing the blood-brain barrier allowing PET imaging of the brain in human subjects.[15] In previous work, we modified the *bis*(thiosemicarbazone) ligand to append substituted stilbenyl functional groups (Figure 3b). These copper(II) complexes bound to amyloid-β plaques in human brain tissue.[16,17] In this work, we prepared copper complexes with *bis*(thiosemicarbazone) ligands incorporating a tetrazine functional group (Figure 3c) designed for bioorthogonal *in vivo* click reactions with the TCO-modified antibodies. Copper(II) complexes of *bis*(thiosemicarbazones) are stable (K_a ~ 10^{18}), [18] but reduction of the metal to copper(I) can lead to dissociation from the ligand and transfer of the copper to proteins that have a high affinity for copper(I). Electron donating methyl or ethyl substituents on the backbone of the ligand (R in Figure 3c) give copper(II) complexes that are more resistant to reduction to copper(I) and can also influence their biodistribution.[19] Two ligands with a benzylaminotetrazine (Tz) functional group with either methyl (H_2atsm-Tz) or ethyl (H_2dtse-Tz) groups were prepared by selective transamination reactions.[20] The copper(II) complexes, Cu(atsm-Tz) and Cu(dtse-Tz) (Figure 3c), were characterised by electrospray mass spectrometry and reverse-phase HPLC. Cyclic voltammetry shows that both Cu(atsm-Tz)

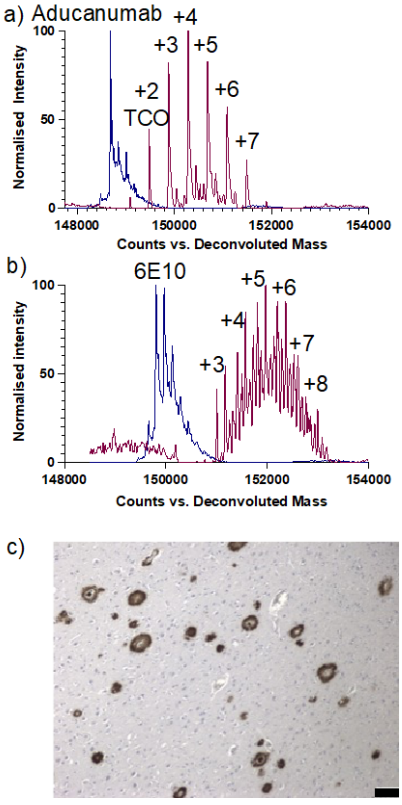

Figure 2 Deconvoluted ESI mass spectra of (a) unconjugated aducanumab (blue) and aducanumab-TCO_x conjugate where x= 2-7 (red); (b) unconjugated 6E10 (blue) and 6E10-TCO_x conjugate where x= 3-8 (red) and (c) section of human brain tissue from AD affected subject immuno-stained with 6E10-TCO antibody; black scale bar = 100 µm.

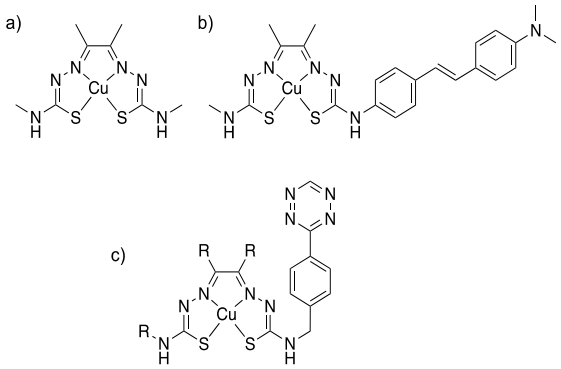

Figure 3 a) Cu(atsm); c) Cu(atsm-stilbene), binds to amyloid-β plaques (previous work)[17] c) Cu(atsm-Tz): R = CH_3; Cu(dtse-Tz): R = CH_2CH_3 (this work).

and Cu(dtse-Tz) undergo a quasi-reversible redox process at $E_{1/2}$ = -1.15 V *vs* ferricenium/ferrocene (Fc^+/Fc) that can be attributed to a $Cu^{II/I}$ process similar to what is found in Cu(atsm) ($E_m \approx -1.16$ V). A second quasi-reversible process at $E_{1/2}$ = -1.32 V is attributed to reduction of the tetrazine functional group. Both the $Cu^{II/I}$ and tetrazine reductions occur at potentials that are outside the typical reducing environment encountered in most cells. Each complex also displayed two essentially irreversible and partially overlapping processes at more positive potentials, i.e., E = 0.19 V vs Fc^+/ Fc which are likely to be due to ligand-based oxidation. Characterisation of Cu(dtse-Tz) by X-ray crystallography (Figure 4a) confirmed the copper(II) is in a distorted square planar environment with the ligand acting as a N_2S_2 donor. The Cu–N bond and Cu-S bond lengths are similar to those found in Cu(atsm).[21] The double deprotonation of the ligand and the resonance form depicted (Figure 3c) is supported by the short C-N lengths (C3-N2 1.323(5) and C6-N5 1.321(5) Å) consistent with partial double bond character.[21] The C-S bond lengths (C3-S1 1.764(4) and C6-S2 1.766(4) Å) are also consistent with more 'thiolate-like' than 'thione-like' bonding.[21] Crystals of protonated $[Cu(H_2atsm\text{-}Tz)]^{2+}$, where the *bis*(thiosemicarbazone) ligand is protonated, were grown by the addition of perchloric acid to a mixture of the complex in methanol (Figure 4b). The most notable differences when comparing to the structure of charge neutral Cu(dtse-Tz) are the longer C-N bond lengths, C2-N1 1.319(4) Å and C2-N2 1.354(4) Å and the shorter C-S bond distances, C2-S1 1.712(3) Å and C5 S2 1.709(3) Å) (Figure 4b). The copper(II) is 5-coordinate square pyramidal due to a weak axial interaction with the oxygen of a perchlorate anion (Cu-O3 2.505(3) Å) (Figure 4b). Despite the change in degree of protonation of the ligand the Cu-N and Cu-S bond lengths are similar to the charge neutral Cu(dtse-Tz).

Both ligands can be radiolabelled with $[^{64}Cu]^{2+}$ in sodium acetate buffer (100 mM, pH 5.5) at room temperature in < 30 minutes to give the copper-64 complexes in high radiochemical yield and specific activity (4.2 - 4.6 MBq/nmol, ESI figure S22, 23). The copper-64 complexes were characterised by comparing their respective HPLC traces with their non-radioactive analogues. The octanol-PBS distribution coefficient (LogD) is often used to predict a compounds ability to cross the blood-brain barrier with the ideal range often stated to be LogD 1.5 - 3.5. The LogD values of $[^{64}Cu]$Cu(atsm-Tz) (LogD 1.84) and $[^{64}Cu]$Cu(dtse-Tz) (LogD 2.17) were consistent with their

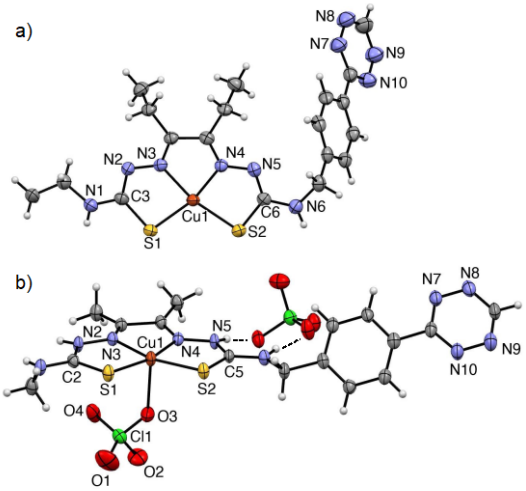

Figure 4 ORTEP representations (with ellipsoids at 50% probability) of the X-ray crystal structures of: a) Cu(dtse-Tz), selected bond lengths (Å): Cu-N3 1.966(3); Cu-N4 1.965(3); Cu-S1 2.2430(11); Cu-S2 2.2453(10). b) $[Cu(H_2atsm\text{-}Tz)](ClO_4)_2$ selected bond lengths (Å): Cu-N3 1.968(3); Cu-N4 1.957(3); Cu-S1 2.2413(8); Cu-S2 2.2489(9); Cu-O3 2.505(3).

respective HPLC retention times and slightly higher than the value obtained for $[^{64}Cu]$Cu(atsm) (LogD 1.56). Both $[^{64}Cu]$Cu(atsm-Tz) and $[^{64}Cu]$Cu(dtse-Tz) were stable with respect to a kinetic challenge experiment with excess of cysteine and histidine at 37 °C for 4 hours, as well as incubation with excess glutathione for 24 hours. (ESI, Figure S13,14,24). Both the initial radiolabelling reactions and the click reactions were analysed by radio-thin layer chromatography (radio-TLC). Unchelated copper-64 stays at the baseline (ethanol mobile phase), while $[^{64}Cu]$Cu(atsm-Tz) and $[^{64}Cu]$Cu(dtse-Tz) travel to the solvent front (Figure 5). Either TCO-aducanumab or TCO-6E10 (~1 equivalent based on the total amount of ligand present with respect to the antibody, ~ 3.6 -3.9 x 10^{-10} mol, 10^{-6}M) were added to $[^{64}Cu]$Cu(atsm-Tz) and $[^{64}Cu]$Cu(dtse-Tz)] and the mixture was allowed to react for 1 hour at room temperature. Analysis of the reaction mixtures by radio-TLC reveals that the majority (> 68 %) of the activity is now retained on the baseline, consistent with copper-64 complexes reacting with the TCO-modified antibodies (Figure 5). When unmodified 6E10 and aducanumab were incubated with both $[^{64}Cu]$Cu(atsm-Tz) and

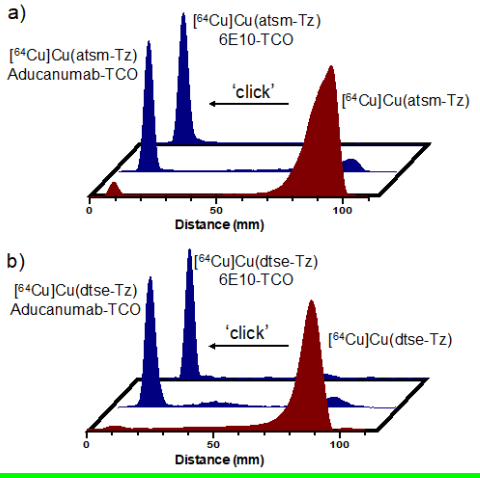

Figure 5 Normalised, smoothed radio-TLC traces of a) $[^{64}Cu]$Cu(atsm-Tz) and b) $[^{64}Cu]$Cu(dtse-Tz) (red) >95% RCY, when reacted with aducanumab-TCO or 6E10-TCO (blue) for 1 h, in 0.1M NaOAc, pH 5.5, 10^{-6}M.

[^{64}Cu]Cu(dtse-Tz), the radioactive signal remained unchanged, consistent with no reaction occurring (ESI, Figure 25, 26).

Encouraged by the efficacy of the click reaction we investigated the potential of the two compounds to cross the blood brain barrier in mice. Following administration of either [^{64}Cu]Cu(atsm-Tz) or [^{64}Cu]Cu(dtse-Tz) to wild type mice by intravenous tail vein injection, the mice were euthanised at 2 and 60 minutes post injection (m.p.i.). The radioactivity in each organ was counted and expressed as a percentage of the injected activity normalised to the mass of the organ (% IA/g). The brain uptake at 2 m.p.i. of [^{64}Cu]Cu(atsm-Tz) was 2.5 ±0.5 % IA/g whilst the brain uptake of [^{64}Cu]Cu(dtse-Tz) was 1.7 ± 0.3 % IA/g. Both compounds clear from the brain in wild type mice with the activity in the brain reducing to 0.78 ± 0.08 % IA/g and 0.41 ± 0.03 % IA/g at 60 m.p.i. For both compounds, the degree of brain uptake in wild type mice is slightly higher than for [^{64}Cu]Cu(atsm) (~0.9 ± 0.4% IA/g).[22] In this experiment, with wild type mice and no TCO-antibody present to 'trap' the tracer it is important that the initial brain uptake is followed by effective clearance. Both [^{64}Cu]Cu(atsm-Tz) and [^{64}Cu]Cu(dtse-Tz) have high uptake in the liver (19.8 ± 1.2 % IA/g and 34.5 ± 3.7 % IA/g respectively at 60 m.p.i.) consistent with hepatobiliary metabolism as would be expected for lipophilic compounds. The initial brain uptake and clearance of [^{64}Cu]Cu(atsm-Tz) was further confirmed by micro-PET imaging, which clearly shows initial brain uptake followed by clearance of the radiotracer (Figure 6).

A challenge in using radiolabelled antibodies for PET imaging of neurodegenerative diseases is the low amounts of antibody that cross the blood-brain barrier. Continued dosing of antibodies modified for bioorthogonal click reactions has the potential to increase the concentration of antibody present in the brain and allow amyloid pre-targeting. To explore this concept, we modified two antibodies, that bind to amyloid-β, with TCO functional groups. We also prepared two new copper-64 complexes with tetrazine functional groups that that cross the blood-brain barrier. These new copper-64 complexes react via bioorthogonal click chemistry with the modified TCO-antibodies. This work suggests that pre-targeting amyloid plaques may be feasible and further investigation of this concept in animal models of amyloid pathology is warranted. Extrapolation of this concept to other antibodies that bind to other proteins of interest in neurodegeneration such as tau, TDP-4 and α-synuclein could be worthy of investigation.

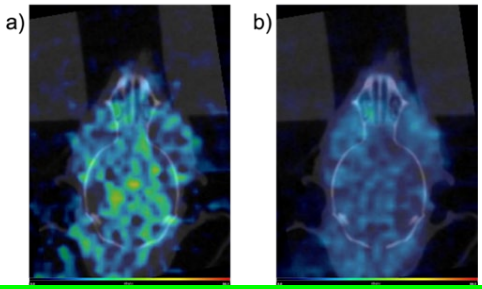

Figure 6. PET/CT images of brain region in Balb/c mouse at a) 1-5 m.p.i. and b) 5-30 m.p.i of [^{64}Cu]Cu(atsm-Tz).

Conflicts of Interest

The Authors declare no conflicts of interest.

Acknowledgments

The Australian Research Council, The Australian Cancer Research Foundation, the Victorian Brain Bank Network, the Mass Spectrometry and Proteomics Facility (Bio21), and the facilities, and scientific and technical assistance of the National Imaging Facility, a National Collaborative Research Infrastructure Strategy capability, at Monash Biomedical Imaging.

Notes and References

1. **D. S. Knopman, H. Amieva, R. C. Petersen, G. Chételat, D. M. Holtzman, B. T. Hyman, R. A. Nixon and D. T. Jones, *Nat. Rev. Dis. Primers.*, 2021, 7, 33.**
2. **B. Dubois, N. Villain, G. B. Frisoni, G. D. Rabinovici, M. Sabbagh, S. Cappa, A. Bejanin, S. Bombois, S. Epelbaum, M. Teichmann, M.-O. Habert, A. Nordberg, K. Blennow, D. Galasko, Y. Stern, C. C. Rowe, S. Salloway, L. S. Schneider, J. L. Cummings and H. H. Feldman, *Lancet. Neurol.*, 2021, 20, 484-496.**
3. C. R. Jack, D. A. Bennett, K. Blennow, M. C. Carrillo, B. Dunn, S. B. Haeberlein, D. M. Holtzman, W. Jagust, F. Jessen, J. Karlawish, E. Liu, J. L. Molinuevo, T. Montine, C. Phelps, K. P. Rankin, C. C. Rowe, P. Scheltens, E. Siemers, H. M. Snyder, R. Sperling, C. Elliott, E. Masliah, L. Ryan and N. Silverberg, *Alzheimers. Demen.*, 2018, **14**, 535-562.
4. F. Panza, M. Lozupone, G. Logroscino and B. P. Imbimbo, *Nat. Rev. Neurol.*, 2019, **15**, 73-88.
5. O. Hansson, *Nat. Med.*, 2021, **27**, 954-963.
6. V. L. Villemagne, V. Doré, S. C. Burnham, C. L. Masters and C. C. Rowe, *Nat. Rev. Neurol.*, 2018, **14**, 225-236.
7. T. Yang, S. Li, H. Xu, D. M. Walsh and D. J. Selkoe, *J. Neurosci.*, 2017, **37**, 152.
8. L. Zhu, K. Ploessl and H. F. Kung, *Chem. Soc. Rev.*, 2014, **43**, 6683-6691.
9. J. Sevigny, P. Chiao, T. Bussière, P. H. Weinreb, L. Williams, M. Maier, R. Dunstan, S. Salloway, T. Chen, Y. Ling, J. O'Gorman, F. Qian, M. Arastu, M. Li, S. Chollate, M. S. Brennan, O. Quintero-Monzon, R. H. Scannevin, H. M. Arnold, T. Engber, K. Rhodes, J. Ferrero, Y. Hang, A. Mikulskis, J. Grimm, C. Hock, R. M. Nitsch and A. Sandrock, *Nature*, 2016, **537**, 50-56.
10. A. Mullard, *Nature*, 2021, **594**, 309-310.
11. R. Rossin, P. Renart Verkerk, S. M. van den Bosch, R. C. M. Vulders, I. Verel, J. Lub and M. S. Robillard, *Angew. Chem. Int. Ed. Engl.*, 2010, **49**, 3375-3378.
12. M. Altai, R. Membreno, B. Cook, V. Tolmachev and B. M. Zeglis, *J. Nucl. Med.*, 2017, **58**, 1553.
13. I. Baghallab, J. M. Reyes-Ruiz, K. Abulnaja, E. Huwait and C. Glabe, *J. Alzheimers. Dis.*, 2018, **66**, 1235-1244.
14. P. J. Blower, *Dalton Trans.*, 2015, **44**, 4819-4844.
15. M. Ikawa, H. Okazawa, K. Arakawa, T. Kudo, H. Kimura, Y. Fujibayashi, M. Kuriyama and M. Yoneda, *Mitochondrion*, 2009, **9**, 144-148.
16. S. Lim, B. M. Paterson, M. T. Fodero-Tavoletti, G. J. O'Keefe, R. Cappai, K. J. Barnham, V. L. Villemagne and P. S. Donnelly, *Chem. Commun.*, 2010, **46**, 5437-5439.
17. A. Noor, D. J. Hayne, S. Lim, J. K. Van Zuylekom, C. Cullinane, P. D. Roselt, C. A. McLean, J. M. White and P. S. Donnelly, *Inorg. Chem.*, 2020, **59**, 11658-11669.
18. Z. Xiao, P. S. Donnelly, M. Zimmermann and A. G. Wedd, *Inorg. Chem.*, 2008, **47**, 4338-4347.
19. C. J. Mathias, S. R. Bergmann and M. A. Green, *J. Nucl. Med.*, 1995, **36**, 1451.
20. B. M. Paterson, J. A. Karas, D. B. Scanlon, J. M. White and P. S. Donnelly, *Inorg. Chem.*, 2010, **49**, 1884-1893.
21. A. R. Cowley, J. R. Dilworth, P. S. Donnelly, E. Labisbal and A. Sousa, *J. Am. Chem. Soc.*, 2002, **124**, 5270-5271.
22. M. T. Fodero-Tavoletti, V. L. Villemagne, B. M. Paterson, A. R. White, Q.-X. Li, J. Camakaris, G. O'Keefe, R. Cappai, K. J. Barnham and P. S. Donnelly, *J. Alzheimers. Dis.*, 2010, **20**, 49-55.

